www.czasopisma.pan.pl PAN POLSKA AKADEMIA NAUK www.journals.pan.pl

PAN ARCHIVES OF ACOUSTICS
Vol. 39, No. 3, pp. 395–402 (2014)

DOI: 10.2478/aoa-2014-0043

Design of Acoustic Tubes Array and Application to Measuring Acoustic Loads in Supersonic Airflow

Long WEI[(1),(2)], Min LI[(1),(2)], Qiang FU[(1),(2)], Yue FAN[(1),(2)], Debin YANG[(1),(2)]

[(1)] *School of Mechanical Engineering, University of Science and Technology Beijing*
30 Xueyuan Road, Haidian District, Beijing 100083, P.R. China; e-mail: limin@ustb.edu.cn

[(2)] *Research Center for Aerospace Vehicles Technology, University of Science and Technology Beijing*
30 Xueyuan Road, Haidian District, Beijing 100083, P.R. China

(*received December 14, 2013; accepted July 8, 2014*)

In the acoustic fatigue experiment for hypersonic vehicle in simulated harsh service environment on ground, acoustic loads on the surface of test pieces of the vehicle need to be measured. However, for the normal microphones without high temperature resistance ability, the near field sound measurement cannot be achieved. In this work, on the basis of previous researches, an acoustic tubes array is designed to achieve the near field measurement of acoustic loads on the surface of the test piece in the supersonic airflow with high temperature achieved by coherent jet oxygen lance. Firstly, the process of designing this acoustic tubes array is introduced. Secondly, the equality of phase differences at the front and at the end of the tubes is stated and proved using a phase differences test with an acoustic tubes array whose design is presented in this text; therefore, the phase differences of signals acquired by microphones can be directly applied to beamforming algorithm to determine the acoustic load source. Finally, using above mentioned acoustic tubes array, measurement of acoustic load, with and without a test piece in the supersonic airflow made by the coherent jet oxygen lance, is conducted respectively, and the measurements results are analyzed.

Keywords: acoustic load, acoustic tubes array, near field measurement, supersonic airflow.

1. Introduction

A hypersonic vehicle works in extremely harsh environment. It faces considerable amount of challenges such as high temperature, noise and aerodynamic loads during its flight. For high intensity of the aerodynamic noise, made by the propulsion system and boundary layer, the random vibration on the wall of the vehicle is excited, and thereby degenerates an acoustic fatigue crack in weak position of the vehicle, leading to fatigue failure (Swanson *et al.*, 2007; Clarkson, 1994; Mixson, Roussos, 1987; NASA, 2001; Moses *et al.*, 2004). Acoustic fatigue has a considerable effect on the service life and the safety of hypersonic vehicles. Thus, when designing the vehicle body some acoustic fatigue experiments on vehicle materials and structures in simulation service environment on ground should be conducted to test their fatigue life. In order to predict the accurate fatigue life, it is necessary to measure the acoustic load on surface of the test piece.

In the past few decades, tremendous progress was made by NASA Langley in the field of experiments on acoustic fatigue in high sound intensity and high temperature. A traveling-wave tube system was designed, where the acoustic load with high sound pressure level (more than 160 dB) could be produced, and a quartz lamp heater was put to heat the test piece. Furthermore, some microphones were mounted on the wall of that tube to monitor the acoustic intensity in this environment. Meanwhile, NASA Langley also conducted acoustic fatigue experiments in a reverberation chamber (Rizzi, 2001; Craig *et al.*, 2007). However, as the acoustic fields in both environments were regarded as uniform acoustic fields, the attention was not focused on the measurement of acoustic loads distribution on surface of the test piece.

In 2009 the US Air Force used a microphone array in near field to characterize the jet noise made by F-22, thus providing a guide for measurement of thermo-acoustic loads distribution. In this measurement, if all

of the microphones were for a long time totally exposed to the jet with high temperature, the temperature of microphones would be increased and even would exceed the temperature limit below which they functioned well. Therefore, a cool down period of 4.5 min was taken during each test script; hence, the total experiment time was increased (National Instrument, 2010). If the thermo stability of microphones were good enough, the cool down period would be maintained. In 2011 a fiber-optical microphone for thermo-acoustic measurements was designed, and it proved to be high temperature resistant (Konle, Paschereit, Röhle, 2011). However, the application of this microphone to measuring acoustic loads with high frequency and intensity was limited. In 2012, to resist high temperature, NASA Langley put a microphone array in a protection chamber for measuring launch vehicle lift-off acoustics (Garcia, 2012), indicating the feasibility of near field measurement made by normal microphones with thermal protection.

Coherent jet oxygen lance was designed, based on the principle of coherent jet in electric furnace steel making, which can jet supersonic airflow with high temperature. The real harsh working condition of material or structure of a hypersonic vehicle can be simulated by this facilities offering the experiment condition on ground (Yang *et al.*, 2007).

In this work, on the basis of previous researches, to achieve the near field measurement of the acoustic loads on the surface of the test piece in the supersonic airflow with high temperature made by coherent jet oxygen lance, an acoustic tubes array is designed. With this array, the sound signals in harsh near field are transmitted to a relative low-temperature place, where a number of normal microphones composing a microphone array are mounted, measuring the sound signals. Thereupon, using these sound signals, the beamforming algorithm is used to measure the distribution and intensity of acoustic load source on surface of the test piece. In this array, the function of the tube is to protect the microphone from the heat area and transmit the sound wave. The suggested acoustic tubes array can be used to achieve the acoustic near field measurement in harsh environment.

In the rest of this article, firstly the process of designing an acoustic tubes array is introduced. Secondly, the equality of phase differences at the front and the back of the tubes is stated and proved by a phase differences test with an acoustic tubes array whose design is presented in this text, therefore the phase differences of signals acquired by microphones can be directly applied to beamforming algorithm to determine the acoustic load source. Finally, using above mentioned acoustic tubes array, measurement of the acoustic load, with and without a test piece in the supersonic airflow made by the coherent jet oxygen lance, is conducted, and the measurements results are analyzed.

2. Design of the acoustic tube

As shown in Fig. 1, in an acoustic field measurement the acoustic wave propagates into the acoustic tube through the entrance, and then to the exit where it is measured by a microphone. The process of designing an acoustic tube includes the choice of a tube diameter, the measuring of eliminating the standing wave, and the installation of the microphone. The details of the process are introduced in the remainder of this section.

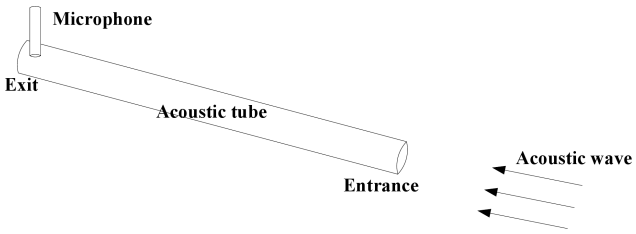

Fig. 1. The acoustic tube.

2.1. The diameter of the acoustic tube

Based on the theory of acoustic tube, the acoustic waves inside a tube are regarded as plane waves which propagate in different directions. However, for an accurate and direct measurement, only the plane wave propagating in the axial direction should exist (Kim *et al.*, 2011). In order to meet that requirements, the diameter d of this tube should satisfy the following formula (Kinsler *et al.*, 1999; Eriksson, 1980)

$$d < 1.841\frac{c}{\pi f}, \tag{1}$$

where c is the minimum sound speed in the tube and f is the cut-off frequency. In this text, the largest frequency of interest is 8000 Hz. Based on the sound speed equation as shown in Eq. (2)

$$c = \sqrt{\frac{\gamma R}{\mu}(273 + t)}, \tag{2}$$

where R, γ and μ are all constants for air, a small air temperature t corresponds to a small value of sound speed. In Eq. (2), $\gamma = 1.402$, $\mu = 29 \times 10^{-3}$ kg/mol, and $R = 8.31$ J/K·mol. Moreover, in the real measurement, the temperature ranges from 10° at the end of the tube, to 64° at the front. Thus, substituting the minimum temperature of 10° into the Eq. (2), the minimum sound speed value in the tube is calculated to be 337.2 m/s. Then based on formula (1), the diameter of the acoustic tube must be less than 24.7 mm. Hence, a kind of tube product with an inner diameter of 22 mm is determined to making the acoustics tube array.

2.2. Elimination of standing wave in the acoustic tube

The standing wave generated by the reflection of sound will distort the sound signal measured by a microphone. In order to eliminate the standing wave a sound-absorbing tube (as long as possible with finite length, called the "semi-infinite tube") is mounted at the end of the acoustic tube. The determination of its parameters depends on the sound deadening capacity TL [dB], which is calculated as the following equation:

$$TL = 4\beta(\alpha)\frac{l}{d_a}, \tag{3}$$

where $\beta(\alpha)$ is the sound deadening ratio, α is the acoustical absorptivity, l represents the length, and d_a is the inner diameter of an semi-infinite tube. The value of $\beta(\alpha)$ can be calculated by Eq. (4)

$$\beta(\alpha) = 4.34 \times \frac{1-\sqrt{1-\alpha}}{1+\sqrt{1+\alpha}}. \tag{4}$$

In this text, the value of TL is intended to reach 60 dB. Next, a kind of rubber tubing product is chosen to be the semi-infinite tube. The value of α is 0.02, the inner diameter d_a is 25 mm, and the length is 18 m. Based on Eq. (4) the value of $\beta(\alpha)$ is 0.021. Later, based on Eq. (3), TL is calculated to be 60.48 dB, which meets the requirements of this text.

2.3. Installation of the microphone

1/2 inch pressure field electret microphone is used in this paper. When mounting a microphone on an acoustic tube, the vertical position of a microphone should be kept as high as possible while ensuring that the whole diaphragm is in the tube, as shown in Fig. 2.

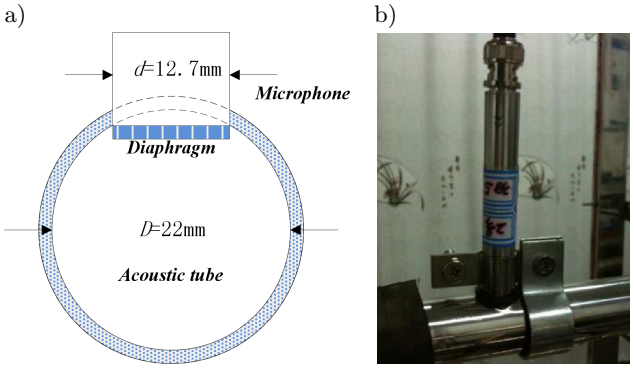

Fig. 2. Installation of a microphone: a) spatial relation between the microphone and acoustic tube, b) the installation picture.

3. Equality of phase differences

Beamforming is a commonly used algorithm for array signal processing that has been widely used in signal source identification (Peral-Orts *et al.*, 2013; Zhao *et al.*, 2013; Bai, Lee, 1998), and the detailed theory of this algorithm can be found in corresponding literature (Markovic *et al.*, 2013; Yan *et al.*, 2009). The essence of beamforming algorithm is that the input signals acquired by all sensors in a sensors array are weighted based on phase differences between the reference sensor and all sensors, and then summed so the output power of the array along the observation direction is enhanced and the one along the other direction is suppressed.

Based on the essence of the beamforming algorithm, during the reconstruction process of acoustic load source distribution by an acoustic tubes array, the key step is the accurate calculation of the phase differences between the phase at the entrance of the reference tube, and that of other tubes. In order to achieve that, the relation between the phase differences at the entrance and those at the exit of the tubes must be determined first.

In fact, based on the theory of acoustic tube, only plane waves parallel to the axial direction propagate in the tube below the cut-off frequency. For a tube x_1 and x_2 stands for the axial position of entrance and exit respectively. Then, the phase difference $\Delta\phi$ between these two positions is calculated as:

$$\Delta\phi = \phi_{x1} - \phi_{x2} = k(x_2 - x_1) = kl, \tag{5}$$

where k is the wave number and l is the distance between these two positions. As a result, for an acoustic tube array with the same tube length, all of the phase differences values of different tubes are equal. Therefore, no matter what the value of $\Delta\phi$ is, the phase differences at the front of the array are the same with those at the end.

In order to prove the equality of phase differences, a 4-element acoustic tubes array is designed based on Sec. 2 in this text for measuring the phase differences in a normal room as shown in Fig. 3a. At the front of the tubes array microphone No. 1 is selected as the reference microphone, then the phase difference between microphone Nos. 2 to 4 and No. 1 is $\Delta\phi_{21}$, $\Delta\phi_{31}$, and $\Delta\phi_{41}$ respectively. Similarly, at the end, microphone No. 5 is the reference microphone, and the phase difference between microphone Nos. 6 to 8 and No. 5 is $\Delta\phi_{65}$, $\Delta\phi_{75}$ and $\Delta\phi_{85}$ respectively.

In the measurement, the distance between the sound source and the acoustic tube is 65 cm. And the distance of each two adjacent tubes is 10 cm. Eight simple tones are produced every a thousand hertz from 1000 Hz to 8000 Hz respectively. The samplings for each frequency are conducted three times. The NI-PXIe system is used to achieve the eight channels of data synchronous acquisition with a sampling frequency of 44100 Hz. The layout of the experiment facilities is shown in Fig. 3b.

By analyzing the cross-correlation between the signals of the reference microphone and those of other

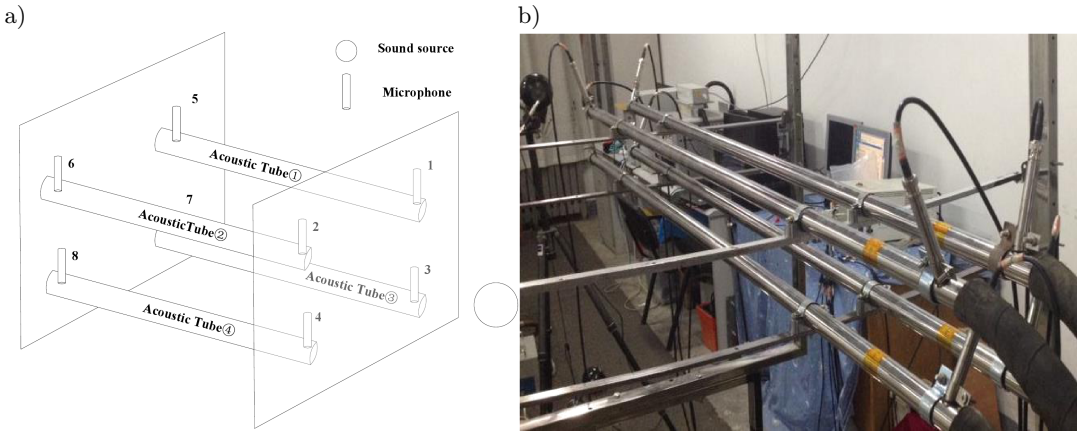

Fig. 3. The layout of the experiment facilities: a) the sketch map, b) the experiment facilities.

microphones, phase differences results are acquired as shown in Table 1. The aim is to observe whether the relation of phase differences shown in Eq. (6) is valid

$$\Delta\phi_{i1} \approx \Delta\phi_{(i+4)5}, \qquad i = 2, 3, 4. \tag{6}$$

In Table 1 the error means the difference between the phase difference at the front of the tubes and at the end, that is to say,

$$error = |\Delta\phi_{(i+4)5} - \Delta\phi_{i1}|, \qquad i = 2, 3, 4. \tag{7}$$

It can be seen that the maximal mean error of all is 0.570 rads in 4000 Hz, which is about 0.09 cycles. That is to say, the value of data offset made by the error is only about one sampling point. Moreover, for most frequencies, the mean error is zero.

In order to further prove the equivalence of phase differences, the sound source maps are plotted by signals of the microphone array at the front and that at the end respectively, based on beamforming algorithm, as shown in Fig. 4 and Fig. 5.

From Figs. 4 and 5, it can be seen that the position of sound source located by the array at the end in each frequency is the same with that by the front array. Thus, it is indicated that the design of sound tubes has good performance in equality between phase differences at the front of the tubes and those at the end. Therefore, phase differences of signals acquired by microphones mounted at the end of tubes can be directly applied to beamforming algorithm without any correction.

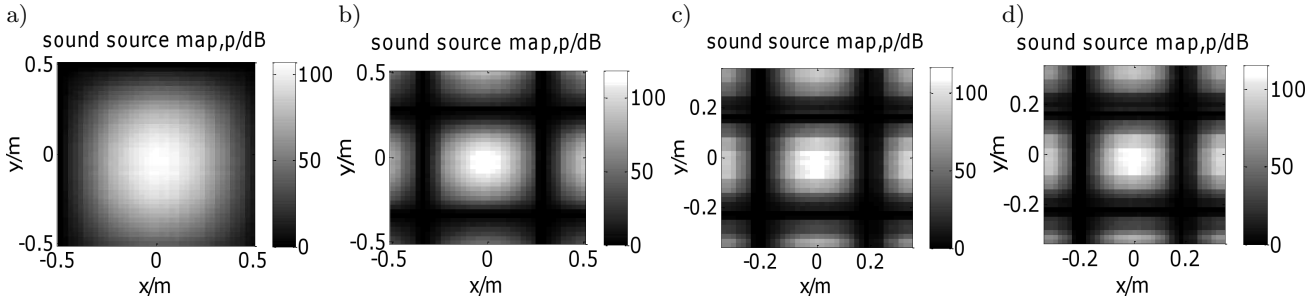

Fig. 4. Sound source maps by the microphone array at the front: a) $f = 2000$ Hz, b) $f = 4000$ Hz, c) $f = 6000$ Hz, d) $f = 8000$ Hz.

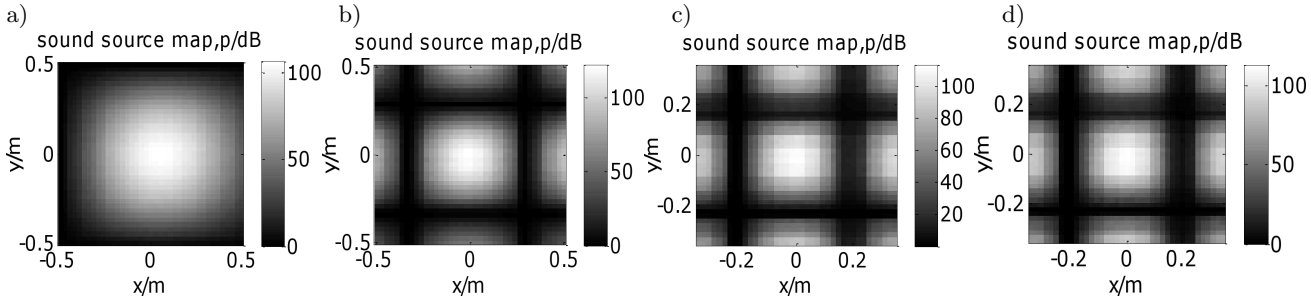

Fig. 5. Sound source maps by the microphone array at the end: a) $f = 2000$ Hz, b) $f = 4000$ Hz, c) $f = 6000$ Hz, d) $f = 8000$ Hz.

Table 1. Comparisons between phase differences at the front and those at the end.

f [Hz]	group	phase difference				phase difference				phase difference			
		$\Delta\phi_{21}$ [rad]	$\Delta\phi_{65}$ [rad]	*error* [rad]	$\overline{error}$ [rad]	$\Delta\phi_{31}$ [rad]	$\Delta\phi_{75}$ [rad]	*error* [rad]	$\overline{error}$ [rad]	$\Delta\phi_{41}$ [rad]	$\Delta\phi_{85}$ [rad]	*error* [rad]	$\overline{error}$ [rad]
1000	1	0	0.142	0.142	0.142	0	0.142	0.142	0.142	0.142	0.142	0.142	0.142
	2	0	0.142	0.142		0	0.142	0.142		0.142	0.142	0.142	
	3	0	0.142	0.142		0	0.142	0.142		0.142	0.142	0.142	
2000	4	0.570	0.570	0	0.190	0.854	0.285	0.569	0.380	0.285	0.285	0	0
	5	0.570	0.285	0.285		0.570	0.285	0.285		0.285	0.285	0	
	6	0.570	0.285	0.285		0.570	0.285	0.285		0.285	0.285	0	
3000	7	0	0	0	0	0	0	0	0	0.427	0.427	0	0
	8	0	0	0		0	0	0		0.427	0.427	0	
	9	0	0	0		0	0	0		0.427	0.427	0	
4000	10	0	0	0	0	0	0.570	0.570	0.570	0	0	0	0
	11	0	0	0		0	0.570	0.570		0	0	0	
	12	0	0	0		0	0.570	0.570		0	0	0	
5000	13	0	0	0	0	0	0	0	0	0	0	0	0
	14	0	0	0		0	0	0		0	0	0	
	15	0	0	0		0	0	0		0	0	0	
6000	16	0	0	0	0	0	0	0	0	0	0	0	0
	17	0	0	0		0	0	0		0	0	0	
	18	0	0	0		0	0	0		0	0	0	
7000	19	0	0	0	0	0	0	0	0	0	0	0	0
	20	0	0	0		0	0	0		0	0	0	
	21	0	0	0		0	0	0		0	0	0	
8000	22	0	0	0	0	0	0	0	0	0	0	0	0
	23	0	0	0		0	0	0		0	0	0	
	24	0	0	0		0	0	0		0	0	0	

4. Measurement in the supersonic airflow

The experiment of measurement of acoustic load is conducted in the environment of supersonic airflow made by coherent jet oxygen lance. The coherent jet oxygen lance system is composed of high pressure air-supply device, central control system, jet system, and measurement section. In this experiment, controlled by central control system, the dimethyl methane, air, and oil are pressurized, and then sent to the pipes of the oxygen lance connected with the atmosphere as shown in Fig. 6. After lighting those three kinds of gases outflowing from the corresponding rings of holes in the oxygen lance, the supersonic airflow with a central temperature of 1200° and a flow velocity of 1.7 Ma, will be generated as shown in Fig. 7.

Fig. 6. The coherent jet oxygen lance.

Fig. 7. The supersonic airflow.

In the experiment, a $310 \times 235 \times 2$ mm rectangle test piece made of aluminium alloy is placed 50 cm away from the oxygen lance. The side of the test piece near the oxygen lance is fixed by the fixture with bolts and the remaining three sides are unfixed. In order to measure the acoustic load source distribution on this test piece in the supersonic airflow, a 3×3 acoustic tubes array, with 100 mm tubes spacing of each two adjacent tubes, is built up 65 cm away from the test piece. The layout of the experiment facilities is shown in Fig. 8. What's more, another experiment to measure the acoustic load in the supersonic airflow without the test piece is conducted. The layout of the test facilities is the same as the former one except for putting away the test piece. NI-PXIe data acquisition system is used to ensure the nine channels data synchronous acquisition.

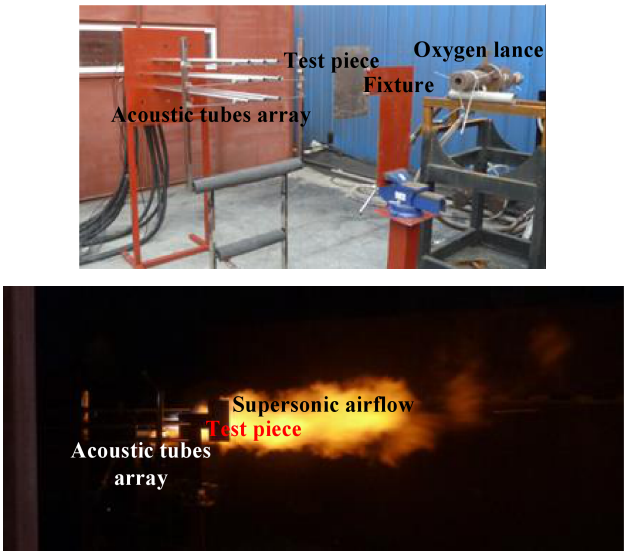

Fig. 8. The layout of the experiment facilities.

The data acquisition starts just a few seconds before the coherent jet oxygen lance begins to work and the whole sampling time is less than 1 minute. Then, all the nine channels of sound signal time domain data is obtained. Observing the time domain data of channel 1 in Fig. 9, it can be seen that in the initial period the amplitude of sound pressure isn't stable because the

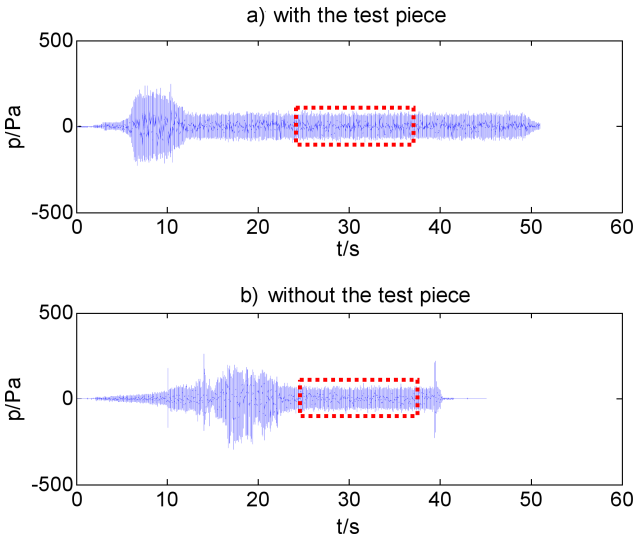

Fig. 9. Sound signal time domain data of channel 1 in two tests.

coherent jet oxygen lance hadn't worked stably since it started. Thus, only the data acquired during the stable period inside the rectangle is applied to the sound load analysis.

In the same running condition of the oxygen lance, the spectrums of the sound signal for channel 1 in the two tests are shown in Fig. 10. Both of spectra can be divided into two parts by the red line. One is the low frequency band and the other is the high frequency band. It can be seen that the dominant frequency band in these two tests is different. For the spectrum without the test piece the dominant frequency band is at the low frequency band part ranging from about 100 Hz to 3000 Hz. On the other hand, for the spectrum with the test piece the dominant frequency band is at the high frequency band part ranging from about 3000 Hz to 5000 Hz. Thus, it is indicated that the change of the dominant frequency band is caused by the test piece.

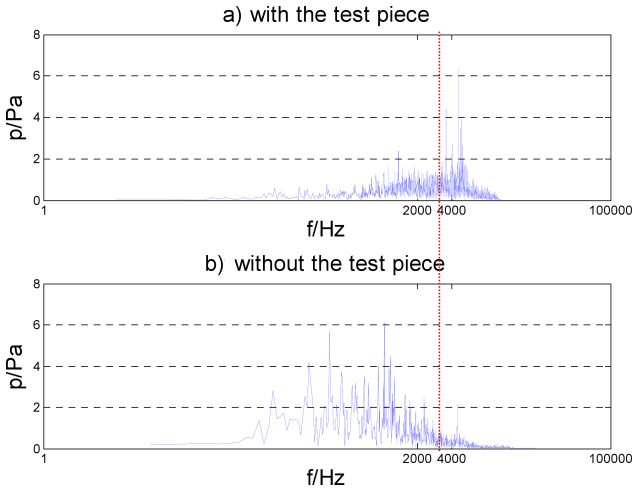

Fig. 10. Spectra of sound signal of channel 1 in two tests.

In order to find out the distribution of the acoustic load source in both high and low frequency bands and further analyze the change of the acoustic load caused by the test piece, acoustic load source maps in those two tests is plotted by beamforming algorithm as shown in Fig. 11 and Fig. 12. In each map, a 1×1 m square is chosen as the analysis area, where the geometric center of the test piece is set as the origin of

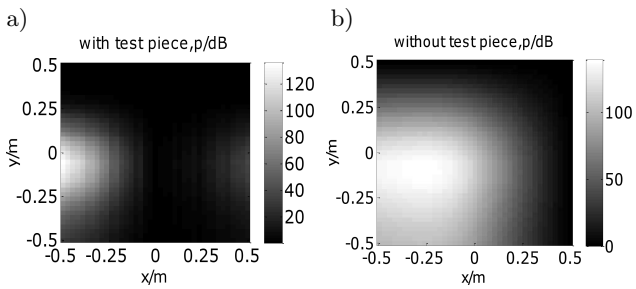

Fig. 11. Acoustic load source maps of the supersonic air flow at low frequency band part: a) with test piece, b) without test piece.

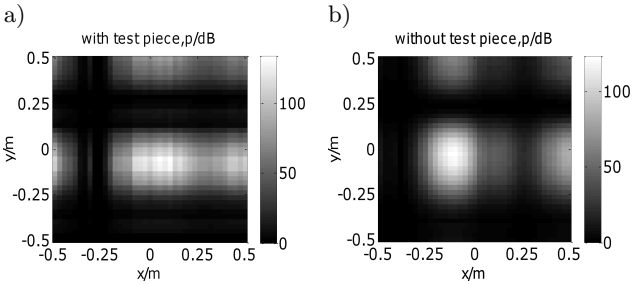

Fig. 12. Acoustic load source maps of the supersonic airflow at high frequency band part: a) with test piece, b) without test piece.

coordinates and the position of the oxygen lance is on the left side. In Fig. 11 the analyzed frequency band is at the low frequency band part ranging from 100 Hz to 3000 Hz which is the dominant frequency band in the test without the test piece. For both tests the acoustic load sources are located near the oxygen lance.

In Fig. 12 the analyzed frequency band is at the high frequency band part ranging from 3000 Hz to 5000 Hz which is the dominant frequency band in the test with the test piece. For the test without the test piece the acoustic load source is still located near the oxygen lance as it is at the low frequency band part. However, for the test with the test piece the acoustic load source is located near the right side of the test piece. From the analysis above, it can be indicated that it is the test piece that changes the original frequency components and the original distribution of acoustic load source in the supersonic airflow. The test piece vibrates under the force of the supersonic airflow. The main frequency component of this vibration probably ranges at high frequency band part. As the right side of the test piece is ufixed, the vibration amplitude there is the most noticeable in the entire test piece and forces the air adjacent the unfixed edge to vibrate intensively. As a result, a new acoustic source of corresponding frequency with large intensity is produced and then measured by the acoustic tubes as shown in Fig. 12a. On the other hand, for the test without the test piece the acoustic load source stays near the oxygen lance whatever the frequency band is. Based on the corresponding literature (Troutt, McLaughlin, 1982) the original acoustic load source in the supersonic airflow should be near the oxygen lance what can explain the test result by the acoustic tubes array.

In conclusion, for the acoustic load distribution of the supersonic airflow without the test piece the dominant frequency band is at low frequency band part and the acoustic load source stays near the jet lance. On the other hand, for the acoustic load distribution of the supersonic airflow with the test piece the dominant frequency band is at the high frequency band part and a new acoustic load source is produced near the unfixed edge of the test piece.

5. Conclusions

1. Aiming at the sound measurement in the supersonic airflow made by the coherent jet oxygen lance, where normal microphones cannot measure directly in the near field, an acoustic tubes array is designed. It not only protects the normal microphones from high temperature but also is applied to acquire the distribution of acoustic load source in the supersonic airflow. This acoustic tubes array could be offered as an alternative method to conduct sound filed measurement in harsh environment.
2. In the environment of a supersonic airflow with a flow velocity of 1.7 Ma and a temperature of 1200° made by the oxygen lance, the acoustic load test, where a test piece is put in the supersonic airflow and that without the test piece, is conducted respectively by the acoustic tubes array. For an accurate reconstruction of the acoustic load source in such an environment, firstly spectrum analysis should be conducted to find out the dominant frequency bands of the sound signal. Next, the beamforming algorithm is used to get the distribution of the acoustic load source in every frequency band separately divided, based on the dominant frequency bands. The test results are analyzed and the effectiveness of using the acoustic tubes array to measure the sound in the supersonic airflow is verified in these tests.

Acknowledgments

This research is supported by the Beijing Higher Education Young Elite Teacher Project (Grant no. YETP0373), the Special-funded Program on National Key Scientific Instruments and Equipment Development (Grant no. 2011YQ14014507) and the Fundamental Research Funds for the Central Universities (Grant nos. FRF-MP-12-002A and FRF-AS-12-003). The authors would also like to express their appreciation to the reviewers for their valuable suggestions and kind work.

References

1. Bai M.R., Lee J. (1998), *Industrial Noise Source Identification by Using an Acoustic Beamforming System*, Journal of Vibration and Acoustics-Transactions of the ASME, **120**, 2, 426–433.
2. Clarkson B.L. (1994), *Review of sonic fatigue technology*, NASA-N94-29407.
3. Eriksson LJ. (1980), *Higher order mode effects in circular duct sand expansion chambers*, J. Acoust. Soc. Am., **68**, 545, 545–550.
4. Garcia R. (2012), *Assessment of Microphone Phased Array for Measuring Launch Vehicle Lift-off Acoustics*, NASA/TM-2012-217563.
5. Kim E.-Y., Kim M.-S., Lee S.-K. (2011), *Identification of the Impact Location in a Gas Duct System Based on Acoustic Wave Theory and the Time Frequency*, Experimental Mechanics, **51**, 6, 947–958.
6. Konle H.J., Paschereit C.O., Röhle I. (2011), *Application of Fiber-Optical Microphone for Thermo-Acoustic Measurements*, Journal of Engineering for Gas Turbines and Power, **133**, 1, doi: 10.1115/1.4001983.
7. Kinsler L.E. *et al.* (1999), *Fundamentals of acoustics*, Wiley, New York.
8. Markovic D., Antonacci F., Sarti A., Tubaro S. (2013), *Soundfield Imaging in the Ray Space*, IEEE Transactions on Audio, Speech, and Language Processing, **21**, 12, 2493–2505.
9. Mixson J.S., Roussos L.A. (1987), *Acoustic fatigue: overview of activities at NASA Langley*, AIAA Dynamics Specialists Conference, Monterey, Calif., 9–10 Apr. 1987, **1**, 9–10.
10. Moses P.L., Rausch V.L., Nguyen L.T., Hill J.R. (2004), *NASA hypersonic flight demonstrators – overview status and future plans*, Acta Astronautica, **55**, 3–9, 619–630.
11. NASA (2001), *Dynamic environmental criteria*, NASA-HDBK-7005.
12. National Instrument (2010), *Jet Engine Noise and Aero-acoustic Noise Measurement*.
13. Peral-Orts R., Velasco-Sanchez E., Campillo-Davó N., Campello-Vicente H. (2013), *Using Microphone Arrays to Detect Moving Vehicle Velocity*, Archives of Acoustics, **38**, 3, 407–415.
14. Rizzi S.A. (2001), *Closed-Loop Control for Sonic Fatigue Testing Systems*, Sound And Vibration, **35**, 11, 19–22.
15. Stephens C.A., Hudson L.D., Piazza A. (2007), *Overview of an Advanced Hypersonic Structural Concept Test Program*, FlAP Annual meeting-hypersonic project, 2007.
16. Swanson A.D., Coghlan S.C., Pratt D.M., Paul D.B. (2007), *Hypersonic vehicle thermal structure test challenges*, AIAA-2007-1670.
17. Troutt T.R., McLaughlin D.K. (1982), *Experiments on the flow and acoustic properties of a moderate-Reynolds-number supersonic jet*, J. Fluid Mech., **116**, 123–156.
18. Yan Shefeng, Ma Yuanliang (2009), *Sensor Array Beampattern Optimization: Theory with Applications*, Science Press, Beijing.
19. Yang Z., Wang Z., Zhu R. *et al.* (2007), *Design and application of coherent jet oxygen lance*, Journal of University of Science and Technology Beijing, **29**, S1, 81–84.
20. Zhao D., Huang Z., Su S., Li T. (2013), *Matched-field Source Localization with a Mobile Short Horizontal Linear Array in Offshore Shallow Water*, Archives of Acoustics, **38**, 1, 105–113.